JOURNAL OF AIRCRAFT
Vol. 36, No. 3, May–June 1999

Lift Prediction of Spanwise Cambered Delta Wings

Lance W. Traub*
Texas A&M University, College Station, Texas, 77843-3141

An analytic prediction method is derived to estimate the lift of delta wings with constant anhedral or dihedral, i.e., a V wing. The method is based on the leading-edge suction analogy, with expressions for leading-edge suction being developed that account for anhedral and dihedral. An empirical correction is combined with the resulting expression to incorporate an effective leading-edge sweep interpretation of wing roll. This approach allows an estimation of the disparate effects of anhedral and dihedral. The attached flow lift component is estimated using a Trefftz plane expression for the apparent mass of a V wing. Comparisons are made with a variety of planforms, with encouraging agreement between theory and experiment being demonstrated.

Nomenclature

AR	= aspect ratio
b	= projected wingspan
C_{Di}	= induced or lift-dependent drag coefficient
C_L	= lift coefficient
C_{Lp}	= potential lift coefficient
C_{Lv}	= vortex lift coefficient
C_T	= leading-edge thrust coefficient
k_i	= induced wing efficiency parameter
k_P	= potential constant
k_V	= vortex lift constant
L	= total lift
m_{22}	= apparent mass coefficient
S	= projected planform area
T	= thrust
U_∞	= freestream velocity
w_i	= velocity induced normal to wing surface by trailing vortex system
w_0	= arbitrary constant
x, y, z	= Cartesian coordinates
α	= wing centerline incidence
Γ	= total effective circulation
γ	= dihedral geometric parameter
ε	= projected wing apex half-angle
Λ	= wing leading-edge sweep angle
Λ_{leag}	= geometric wing leading-edge sweep angle
ρ	= density
ϕ	= wing dihedral angle, defined (−) for anhedral, (+) for dihedral

Subscripts

e	= effective
np	= nonplanar
np-pol	= nonplanar based on Polhamus' method
np-purv	= nonplanar based on Purvis' method
pl	= planar
pr	= projected

Introduction

RAPID prediction methodologies for preliminary design or parametric studies of slender wings are typically based on either the leading-edge suction analogy of Polhamus,[1] or the nonlinear vortex lattice method[2,3] (NLVLM). Both methodologies usually use a vortex lattice (VLM) representation of the wing, with the suction analogy calculating the lift-dependent drag to determine the wing leading-edge suction. This suction is then used to estimate the vortex lift. The NLVLM releases load-free vortex filaments from the wing leading edge that convect downstream, rolling-up in the process and inducing additional velocities on the upper wing surface that account for the leading-edge vortex effects.

The basic tenet of Polhamus's[1] leading-edge suction analogy is that the lift induced on the wing by the separated leading-edge vortices is equal to the theoretical leading-edge suction that would have been developed if the wing profile were suitably contoured. The leading-edge suction force is thus assumed to have been rotated through 90 deg to supplement the normal force. Commonly used implementations of the leading-edge suction analogy[4] predict similar results for wing anhedral/dihedral, a result not seen experimentally. This difference may be due to a simplified representation of the wing boundary conditions such that they are not imposed on the wing surface, but in the x–y plane: planar-equivalent boundary conditions. Enforcement of the boundary conditions on the wing surface would result in anhedral and dihedral inducing dissimilar side wash due to the trailing vortices on both the wing's bound and trailing vortices. In addition, the bound vortices would also induce different backwash on the wing's bound vortices for anhedral and dihedral. Whether the inclusion of these additional effects would result in the suction analogy, VLM correctly predicting the performance of deltas with anhedral/dihedral is uncertain.

An investigation of the NLVLM by Rusak et al.,[5] and a subsequent comment by Luckring,[6] suggest that although this method is a useful tool, its sensitivity to grid refinement in terms of wake vortex length to wing panel length may make accurate force predictions somewhat arbitrary.

Smith[7] developed a flow model for slender wings with leading-edge separation, where the separated flow was approximated as being conical and the attached flow component was found using slender wing theory. The solution was determined in a crossflow plane, using a conformal transformation. Naturally, Smith's slender wing theory is limited by its conical flow assumption in that the effect of the wing trailing edge due to enforcement of the Kutta condition is not considered. This method may, however, provide representative loading and structure near the wing's apex region. Overall forces would be overestimated substantially.

Euler and Navier–Stokes solvers are capable of determining the effect of spanwise camber on delta wings, but are computationally expensive, and not really viable for preliminary or parametric design studies. Further, they do not give an explicit relationship between the design variables, e.g., Λ and ϕ.

Consequently, to extend the utility of the leading-edge suction analogy, a simple analytic prediction method is derived to estimate the lift of delta wings with constant anhedral or dihedral, such that in a crossflow plane, for dihedral, the wing resembles a V. The method is based on the leading-edge suction analogy with expressions for

Received July 23, 1998; revision received Dec. 28, 1998; accepted for publication Dec. 29, 1998.

*Graduate Student, Aerospace Engineering Department. Associate Member AIAA.

leading-edge suction being developed that account for nonplanar effects. An empirical correction is combined with the resulting expression to incorporate Ericsson's[8] effective leading-edge sweep interpretation of wing roll. This procedure allows an estimation of the disparate effects of anhedral and dihedral. The attached flow lift component is estimated using a Trefftz plane expression by Letcher[9] for the apparent mass of a V wing. Anhedral/dihedral effects are determined for a wing with a constrained wingspan, such that increasing nonplanarity changes the wing arc length, but not the span. Numerous comparisons of the method with experimental data are presented for validation.

Discussion of Method

It is common in prediction methods based on slender wing theory or the leading-edge suction analogy to decompose lift into two components. One is due to attached or potential flow and the other comprises the nonlinear vortex lift. Thus, to predict the lift of a nonplanar slender delta wing, it is necessary to estimate these two components.

The following methodology follows that of the Polhamus[1] suction analogy due to the accuracy and flexibility of this method. Polhamus decomposes lift as follows:

$$C_{Lp} = k_P \cos^2\alpha \sin\alpha \tag{1}$$

This expression gives the attached flow or potential lift component in the absence of any leading-edge thrust. The vortex lift is given by

$$C_{Lv} = k_V \cos\alpha \sin^2\alpha \tag{2}$$

and is assumed equal to the leading-edge suction that would have been developed in the absence of leading-edge separation. The total lift is given by $C_{Lp} + C_{Lv}$.

Potential Lift

If a body is accelerated, it experiences a positive pressure in front and a negative pressure to the rear, resulting in a force that resists motion. The body thus behaves as though it had an additional mass. Jones[10] used apparent mass theory to estimate the lift on a slender wing at low α, by assuming that the increasing width, and consequently, scale of the flow of a delta wing penetrating a fixed reference plane requires a lift force equal to the downwash velocity $U_\infty\alpha$; i.e., the relative velocity of the surrounding fluid multiplied by the increase of the apparent mass. Thus, the lift per unit length of the wing is given by

$$\frac{\mathrm{d}L}{\mathrm{d}x} = U_\infty^2 \alpha \frac{\mathrm{d}}{\mathrm{d}x}(m_{22}) \tag{3}$$

where m_{22} is the apparent mass coefficient of the body. Letcher[9] gives an expression for the apparent mass of a V wing, which has been analytically integrated by Smith,[7] and is given by Lowson[11] as

$$m_{22} = \frac{\rho\pi b^2}{4\cos^2\phi}\left(\frac{1-\gamma}{\gamma}\right)^{(2\gamma-1)} \tag{4}$$

where b is the projected wingspan and

$$\gamma = (\pi/2 - \phi)/\pi \tag{5}$$

The total lift is

$$L = \int_0^x \frac{\mathrm{d}L}{\mathrm{d}x}\,\mathrm{d}x \tag{6}$$

which, after the substitution of Eqs. (3) and (4) and upon integration, yields

$$L = \frac{U_\infty^2 \alpha\rho\pi b(x)^2}{4\cos^2\phi}\left(\frac{1-\gamma}{\gamma}\right)^{(2\gamma-1)} \tag{7}$$

Nondimensionalizing by $1/2\rho U_\infty^2 S$ gives the nonplanar potential lift-curve slope as

$$k_{\mathrm{Pnp}} = \frac{\pi\,\mathrm{AR}_{\mathrm{pr}}}{2\cos^2\phi}\left(\frac{1-\gamma}{\gamma}\right)^{(2\gamma-1)} \tag{8}$$

Notice that for a planar wing, where $\gamma = \frac{1}{2}$ and $\phi = 0$ deg, Jones's[10] expression for the lift-curve slope of a slender delta wing is recovered, i.e., $k_{\mathrm{Ppl}} = \pi\,\mathrm{AR}/2$. The accuracy of Jones's expression is typically limited to wings for which $\mathrm{AR} < 0.5$. Equation (8) may be generalized by interpreting it as being composed of a lift-curve slope for a projected planar delta wing ($\pi\,\mathrm{AR}_{\mathrm{pr}}/2$), multiplied by a term to account for nonplanarity of the wing $\{[(1-\gamma)/\gamma]^{(2\gamma-1)}/\cos^2\phi\}$. A more general, or less-restricted expression for the lift-curve slope of a planar delta wing is derived in Ref. 12, and in the present nomenclature is given by $k_{\mathrm{Ppr}} = 4\tan^{0.8}\varepsilon, 0 < \mathrm{AR} < 2$. The potential constant, or attached flow lift-curve slope, for a nonplanar delta wing may thus be expressed as

$$k_{\mathrm{Pnp}} = \frac{4\tan^{0.8}\varepsilon}{\cos^2\phi}\left(\frac{1-\gamma}{\gamma}\right)^{(2\gamma-1)} \tag{9a}$$

or, more generally,

$$k_{\mathrm{Pnp}} = \frac{k_{\mathrm{Ppr}}}{\cos^2\phi}\left(\frac{1-\gamma}{\gamma}\right)^{(2\gamma-1)} \tag{9b}$$

where k_{Ppr} may be found using any appropriate lifting surface theory. Using the apparent mass formulation of Letcher,[9] which was derived in the Trefftz plane (a crossflow reference plane located downstream at infinity), results in k_{Pnp} being equal for anhedral or dihedral. This equality results because the formulation is essentially two dimensional or equivalent to that from slender wing theory in that a crossflow plane is used for solution evaluation and does not take account of any chordwise flow variations. Using a planar equivalent, i.e., enforcing the boundary conditions in the x–y plane, of the wing no-penetration boundary condition, which is often implemented for simplicity in VLM codes, would also result in k_{Pnp} showing symmetry for anhedral/dihedral. Anhedral and dihedral will result in unequal variations in k_{Pnp} due to bound vortex-induced backwash, and trailing vortex-induced sidewash causing loads on both inclined bound vortex elements and the trailing vortices. Nonetheless, as will be clearly shown by the experimental data, the effect of anhedral/dihedral on k_{Pnp} is extremely weak for the range of configurations studied, which coincides with the range of applicability of the prediction method, justifying the use of a simplified representation of k_{Pnp}.

Vortex Lift

The traditional implementation of the leading-edge suction analogy in a panel method would show symmetrical prediction of vortex lift for both anhedral and dihedral. This is as a result of the thrust distribution being determined from the attached-flow VLM solution, which yields similar results for equivalent anhedral or dihedral, as discussed previously. As will be demonstrated, experimental data for spanwise cambered wings show marked differences in the flow for anhedral and dihedral at moderate- to high-lift coefficients. Anhedral has the effect of increasing lift, whereas dihedral generally attenuates lift. These effects are also present on rolled deltas, where the windward wing half experiences higher vortex-induced suction peaks and an earlier onset of vortex breakdown than the leeward wing half. Stephen[13] has shown that the concept of an effective leading-edge sweep can be used to correlate vortex breakdown data for rolled deltas. The effect of wing dihedral can be interpreted as comprising an effective change of wing leading-edge sweep for a given wing centerline incidence. Consequently, anhedral decreases wing sweep and dihedral increases wing sweep. This concept is incorporated in the following analysis. Applying the Kutta–Joukowski

theorem using velocity components normal to the wing chord plane gives the wing leading-edge thrust as

$$T = \rho(U_\infty \sin\alpha \cos\phi - w_i)\Gamma_{np} b \tag{10}$$

Furthermore, $L_{np} = \rho U_\infty \Gamma_{np} b$; thus, $C_{Lnp} = 2\Gamma_{np} b/U_\infty S$ with $C_{Lnp} = k_{Pnp} \sin\alpha$, giving

$$\Gamma_{np} = U_\infty S k_{Pnp} \sin\alpha / 2b \tag{11}$$

where k_{Pnp} is the potential constant for the nonplanar wing. If the wake trace is considered to descend as a rigid surface at w_0, the component of induced velocity normal to the wing surface for no penetration is

$$w_i = w_0 \cos\phi \tag{12}$$

Substituting Eq. (11) into Eq. (10) and nondimensionalizing gives

$$C_T = [\cos\phi - (w_i/U_\infty \sin\alpha)] \sin^2\alpha k_{Pnp} \tag{13}$$

Following Polhamus,[1] $w_0/U_\infty \sin\alpha = k_{Pnp} k_i = k_{Pnp} \partial C_{Di}/\partial C_L^2$, and using Eq. (12) yields

$$C_T = (1 - k_{Pnp} k_i) k_{Pnp} \cos\phi \sin^2\alpha \tag{14}$$

Equation (14) shows that the vortex lift ($=C_T/\cos\Lambda$) for a given wing may be enhanced by increasing the wing lift-curve slope k_{Pnp}, or improving its efficiency k_i, through a reduction in induced drag. To determine k_i, an expression from Letcher[9] for the induced drag may be used:

$$C_{Di} = \tfrac{1}{4}(\rho S/m_{22}) C_L^2$$

which, upon substitution, gives

$$\frac{\partial C_{Di}}{\partial C_L^2} = k_i = \frac{\cos^2\phi}{\pi \mathrm{AR}_e} \left(\frac{\gamma}{1-\gamma}\right)^{(2\gamma-1)} \tag{15}$$

For a planar wing, Eq. (15) reduces to the result of Jones,[10] showing that the wing has elliptic loading. Thus, the thrust may be expressed as

$$C_T = \left[k_{Pnp} - k_{Pnp}^2 \frac{\cos^2\phi}{\pi \mathrm{AR}_e} \left(\frac{\gamma}{1-\gamma}\right)^{(2\gamma-1)}\right] \cos\phi \sin^2\alpha \tag{16}$$

For a planar wing, $\phi = 0$ deg and $\gamma = 0.5$, resulting in this expression being analogous to Polhamus's[1] Eq. (10). As mentioned previously, potential theory would yield equivalent variations in k_{Pnp} and k_i for anhedral or dihedral. Furthermore, the experimental data show that the effect of wing nonplanarity is small at low lift coefficients, suggesting that the effect of anhedral/dihedral is mostly confined to the vortex lift. As a result, Eq. (16) requires an empirical modification to reflect the experimental trends, which comprises altering the induced efficiency term to incorporate expressions for effective leading-edge sweep. An increase in vortex lift [noting that the variation in k_{Pnp} and k_i with ϕ as given by Eq. (9) and Eq. (15), respectively, and demonstrated experimentally, is weak] within the framework of Eq. (16) necessitates an effective increase in wing efficiency, which manifests as an increase in the wing's aspect ratio. Following Ericsson,[8] the effective leading-edge sweep is given by

$$\Lambda_e = \Lambda_{leag} \pm \tan^{-1}(\tan\alpha \sin\phi) \tag{17}$$

where (+) corresponds to dihedral and (−) to anhedral, resulting in an effective aspect ratio given by

$$\mathrm{AR}_e = 4 \tan(\pi/2 - \Lambda_e) \tag{18}$$

The vortex lift constant for the wings under consideration may be expressed as

$$k_V = \frac{\partial C_T \cos\phi}{\partial \sin^2\alpha \cos\Lambda_{leag}}$$

giving

$$k_{Vnp} = \left[k_{Pnp} - k_{Pnp}^2 \frac{\cos^2\phi}{\pi \mathrm{AR}_e} \left(\frac{\gamma}{1-\gamma}\right)^{(2\gamma-1)}\right] \frac{\cos^2\phi}{\cos\Lambda_{leag}} \tag{19}$$

where Λ_{leag} is the actual wing leading-edge sweep (not projected), and is given by

$$\Lambda_{leag} = \pi/2 - \tan^{-1}(\tan\varepsilon/\cos\phi) \tag{20}$$

where ε is the apex half-angle of the projected wing. For $\alpha >$ 20–25 deg, Polhamus'[1] formulation generally results in an overprediction of lift compared with experiment. Purvis[14] derived an alternative expression for k_{Vpl}, which is given by

$$k_{Vpl} = \left(k_{Ppl} \cos^2\alpha - \frac{k_{Ppl}}{\pi \mathrm{AR}} \cos^5\alpha\right) \frac{1}{\cos\Lambda} \tag{21}$$

This expression results in improved accord between theory and experiment at high α, but is virtually identical to Polhamus'[1] k_{Vpl} expression at moderate α. Comparing Eqs. (21) and (19) for $\phi = 0$ deg and $\gamma = \frac{1}{2}$, i.e., a planar wing, shows that Purvis's[14] formulation would result in Eq. (19) being of the form

$$k_{Vnp\text{-}purv} = \left[k_{Pnp} \cos^2\alpha - k_{Pnp}^2 \frac{\cos^2\phi}{\pi \mathrm{AR}_e} \left(\frac{\gamma}{1-\gamma}\right)^{(2\gamma-1)} \cos^5\alpha\right] \times \frac{\cos^2\phi}{\cos\Lambda_{leag}} \tag{22}$$

The final expressions for the lift of a nonplanar delta with constant ϕ are

$$C_{Lnp\text{-}pol} = k_{Pnp} \cos^2\alpha \sin\alpha + \left[k_{Pnp} - k_{Pnp}^2 \frac{\cos^2\phi}{\pi \mathrm{AR}_e} \left(\frac{\gamma}{1-\gamma}\right)^{(2\gamma-1)}\right] \times \frac{\cos^2\phi \sin^2\alpha \cos\alpha}{\cos\Lambda_{leag}} \tag{23}$$

$$C_{Lnp\text{-}purv} = k_{Pnp} \cos^2\alpha \sin\alpha + \left[k_{Pnp} \cos^2\alpha - k_{Pnp}^2 \frac{\cos^2\phi \cos^5\alpha}{\pi \mathrm{AR}_e} \times \left(\frac{\gamma}{1-\gamma}\right)^{(2\gamma-1)}\right] \frac{\cos^2\phi \sin^2\alpha \cos\alpha}{\cos\Lambda_{leag}} \tag{24}$$

where Eq. (23) follows the formulation of Polhamus[1] in the determination of the vortex lift, whereas Eq. (24) follows the formulation of Purvis.[14] The accuracy of Eqs. (23) and (24) will be evaluated subsequently.

Experimental Study

The majority of the experimental data presented in this paper is part of a larger research effort on the effects of spanwise camber on delta wings. As the experimental findings will be reported in a later study, their means of acquisition is described only briefly. The test wings were manufactured from 1.6-mm-thick steel plate and had a root chord of 375 mm. The wings were bent to the desired anhedral/dihedral angle, with the wingspan constrained to produce the desired Λ_{pr}. Thus, the wing's arc length varied. The force balance results were acquired using a six-component Aerolab sting balance. Repeatability of the balance for lift is estimated at $\Delta C_L = 0.0008$. Angle of attack can be set to within 0.05 deg. The output of the balance was acquired using a 16-bit A/D board with each channel being sampled 1000 times and averaged. The results were nondimensionalized using the projected wing area of the respective planform. The tests were run at a root chord Re number of 1.14×10^6. The experimental data were acquired in Texas A&M University's 3×4 ft continuous wind tunnel.

Comparison with Experiment

Application of the suction analogy is limited by the onset of vortex breakdown at the wing trailing edge (BD–TE) as wing AR increases, and by the occurrence of either asymmetric vortices or incomplete upper surface flow reattachment as the wing AR $\rightarrow$ 0, depending on the wing leading-edge geometry for finite thickness wings. For a given α and Λ_{pr}, it follows from the effective sweep concept that increasing anhedral, which reduces effective sweep, should promote the earlier onset of BD–TE. Increasing dihedral, in contrast, should induce either vortex asymmetry or incomplete upper surface flow reattachment.

The application of the suction analogy may be limited by incomplete flow reattachment on the upper wing surface for very low AR wings, violating the assumptions implicit in Polhamus' formulation. Flow reattachment may be affected by the formation of a singularity in the crossflow plane, limiting the quantity of fluid captured and accelerated downward by the vortices. The appearance of asymmetric vortices before the onset of vortex breakdown has been determined to be an artifact of the wing apex crossflow profile as shown by Stahl et al.[15] and others.[16] For slender deltas with thin sharp cross sections, experimental data[15,16] suggests that asymmetry may not manifest on these wings.

The present experimental data were determined for thin wings that were blunt edged. It is thus possible, but unlikely, that the present experimental data were affected by asymmetry. An asymmetry boundary as presented in Ref. 6 may fortuitously be coincident with incomplete upper surface flow reattachment that violates the analogy, although it would be expected that this would result in lift overprediction, which, as will be shown, is not the case. To determine if the application of the asymmetry boundary in terms of AR_e [Eq. (18)] coincides with the observed discrepancy for some dihedral cases between the present prediction method and experiment, this boundary, where present, is included in the data presentation. Figure 1, adapted from Ref. 6, displays a redesignated consolidated experimentally determined asymmetry boundary. As it is unlikely that asymmetry actually manifested on the tested wings, the leftmost boundary in Fig. 1 (originally the asymmetry boundary) may be more accurately construed as an empirically determined applicability boundary for the present method. As will be seen, the asymmetry boundary generally describes the limits of applicability of the present methodology adequately for dihedral, even if it does not describe the actual flow physics.

As previously mentioned, Stephen[13] used the concept of effective leading-edge sweep to correlate vortex burst trajectories for rolled deltas. His analysis suggested that the effective sweep concept, although successful, tended to reduce in predictive accuracy for the leeward wing half at high roll angles. The leeward wing half is analogous to a delta with dihedral and may indicate that the effective sweep concept breaks down for particular combinations of sweep and dihedral.

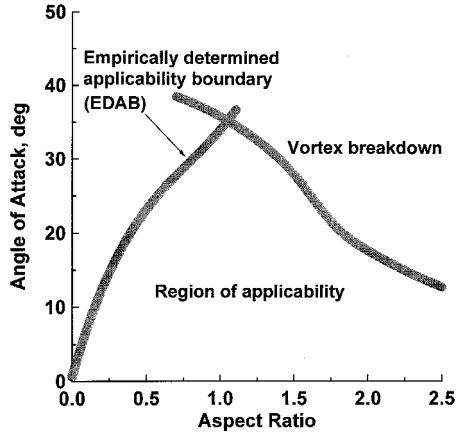

Fig. 1 Semi-empirical applicability boundaries for the present method based on data presented in Ref. 6.

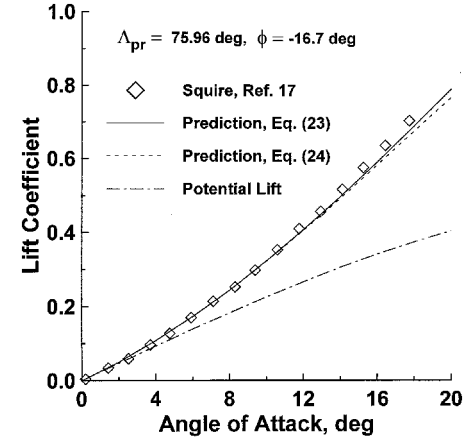

Fig. 2 Comparison of theory and experiment, anhedral.

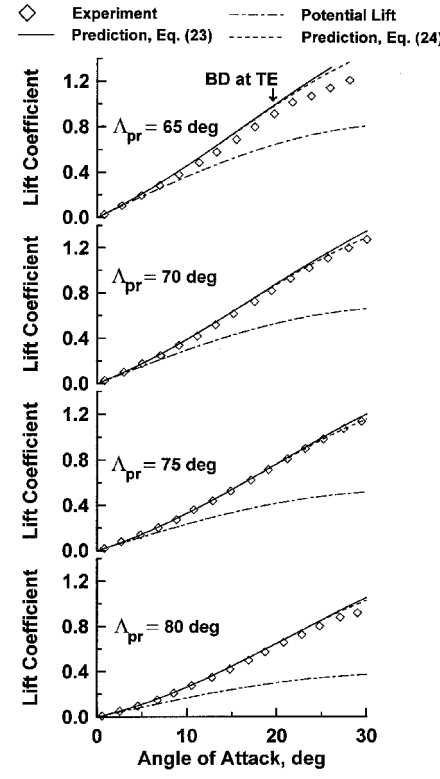

Fig. 3 Comparison of theory and experiment, planar wings.

Comparisons follow with the experimental data determined in the present study, and with the results of Squire.[17] Squire determined the properties of a slender sharp delta, with a projected AR of 1. The wing had an anhedral angle of 16.7 deg. Figure 2 shows comparisons between theory and experiment. The predictions show close accord with the experimental data. Figures 3–11 present comparisons between the prediction method and the present experimental results for $\Lambda_{pr} = 65$ to 80 deg, and $\phi = -25$ to 25 deg with $\Delta\Lambda_{pr}$, and $\Delta\phi$ varying in 5-deg increments. Where appropriate, the semi-empirical limiting boundaries of the suction analogy or effective sweep concept have been indicated in the figures. Figure 3 shows comparisons between Eqs. (23) and (24), which for this case reduce to Polhamus's[1] and Purvis's[14] method and experiment for planar wings. This figure is presented to validate the present experimental data, as for planar sharp-edged delta wings, the suction analogy shows excellent agreement with experiment. Agreement is seen to be excellent, also at high α, Polhamus's[1] formulation tends to slightly overpredict the lift. Figures 4–11 show that for the cases cited, anhedral effects are accurately predicted. For more highly swept wings, the accord between theory and experiment is seen to degrade with increasing wing

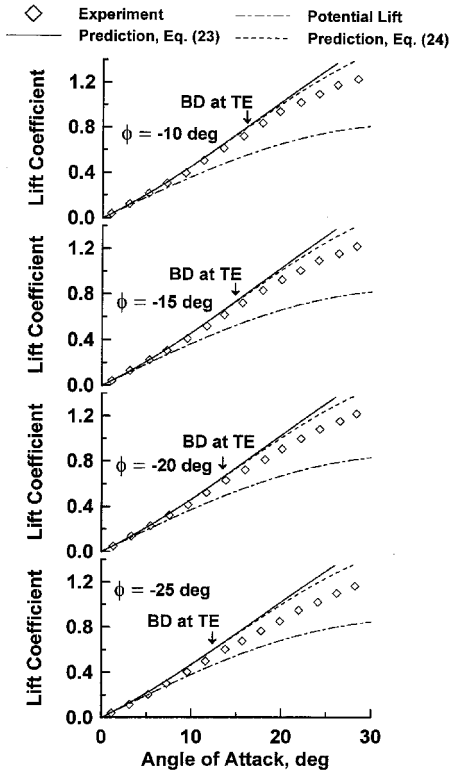

Fig. 4 Comparison of theory and experiment, $\Lambda_{pr} = 65$ deg, anhedral.

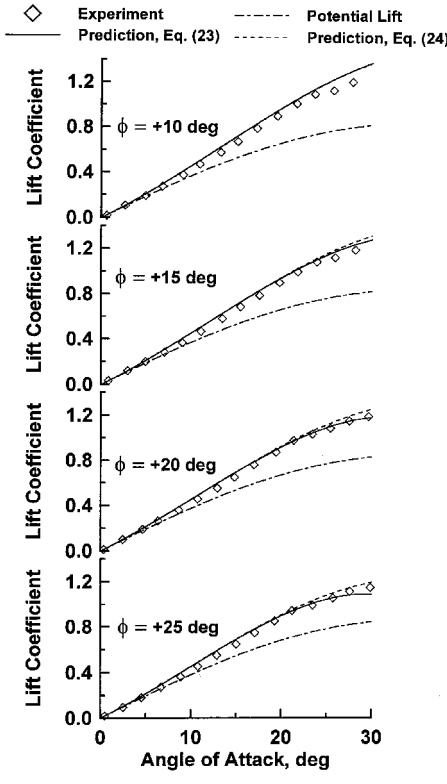

Fig. 5 Comparison of theory and experiment, $\Lambda_{pr} = 65$ deg, dihedral.

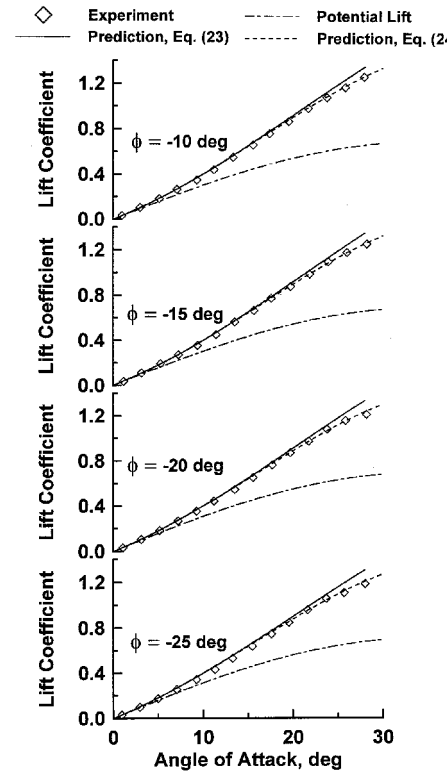

Fig. 6 Comparison of theory and experiment, $\Lambda_{pr} = 70$ deg, anhedral.

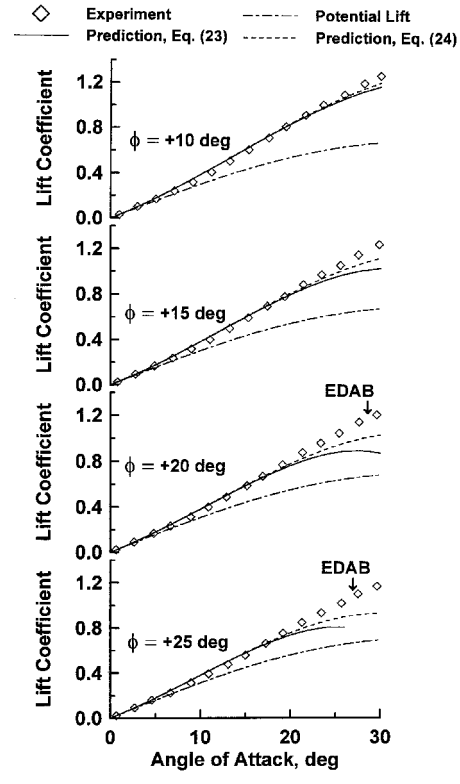

Fig. 7 Comparison of theory and experiment, $\Lambda_{pr} = 70$ deg, dihedral.

dihedral. The empirically determined applicability boundary, based on vortex asymmetry, roughly coincides with the observed deterioration of the predictions. The figures also show that the formulation based on Purvis's[14] method [Eq. (24)] generally shows better agreement with experiment than Eq. (23) based on Polhamus's method.

Figures 12 and 13 exhibit the variation of wing lift coefficient with ϕ for wing centerline incidences of 14 and 20 deg. The dependence of lift on ϕ, particularly for the case of anhedral, is seen to be well predicted. However, at $\alpha = 20$ deg, for $\Lambda_{pr} = 75$ and 80 deg, lift is underpredicted for the dihedral case.

Figure 14 shows the theoretical effects of anhedral on the lift components of the various wing configurations. Analysis of Eqs. (23) and (24) and Fig. 14 shows that anhedral results in a moderate and smooth increase in potential lift C_{Lp} for a given α. The increase in the potential lift coefficient is greater as the wing leading-edge sweep reduces, as a result of the increase in the projected wing's

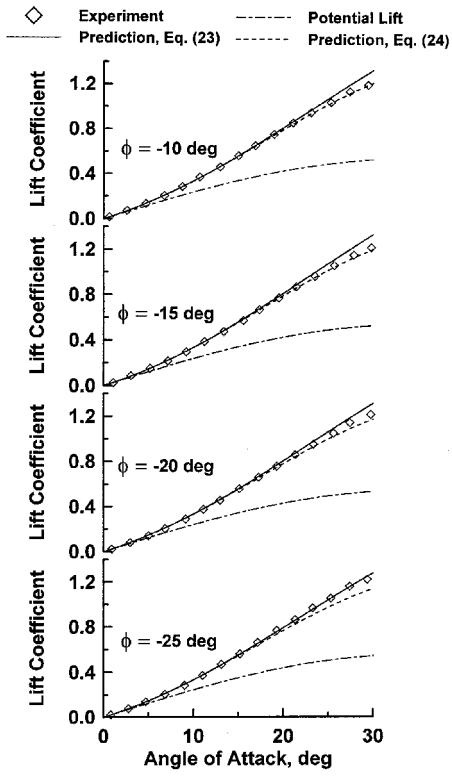

Fig. 8 Comparison of theory and experiment, $\Lambda_{pr} = 75$ deg, anhedral.

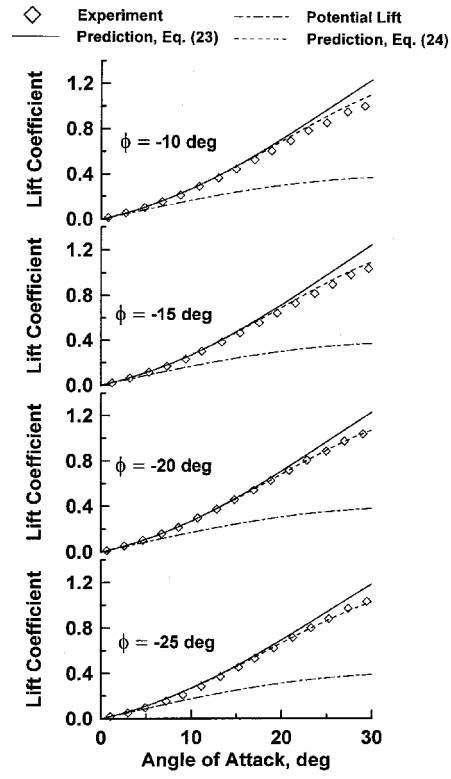

Fig. 10 Comparison of theory and experiment, $\Lambda_{pr} = 80$ deg, anhedral.

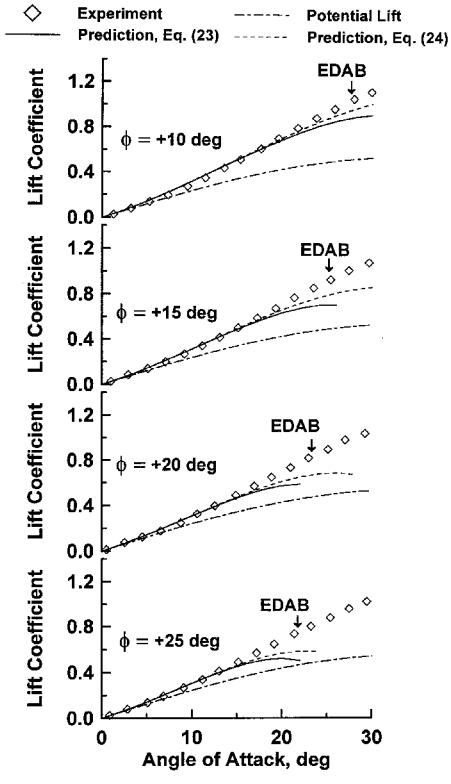

Fig. 9 Comparison of theory and experiment, $\Lambda_{pr} = 75$ deg, dihedral.

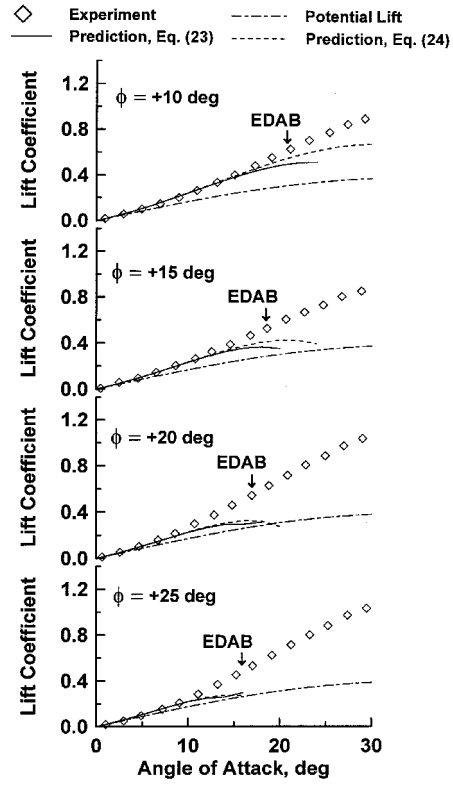

Fig. 11 Comparison of theory and experiment, $\Lambda_{pr} = 80$ deg, dihedral.

lift-curve slope. The relative (not actual magnitude) increase of C_{Lp} with anhedral is, however, independent of sweep. For planar delta wings, the vortex lift developed is often assumed to be relatively independent of sweep with the approximation of $k_{Vpl} = \pi$ often used. The present analysis suggests that the effect of anhedral is such that increasing Λ_{pr} for a given anhedral angle ($\phi \neq 0$ deg) results in a noticeable increase in k_{Vnp}, and, hence, vortex lift. Figure 14 suggests that the maximum vortex lift increase occurs for $\phi = -10$ to -15 deg, depending on Λ_{pr}. For moderate sweep, $\Lambda_{pr} = 65$ deg, ϕ has a small effect on C_L as the vortex lift is weakly affected initially and reduces for anhedral angles greater than 10 deg, whereas the potential lift increases steadily with increasing anhedral. The net effect is that for this wing, anhedral has a moderate impact on the lift generated by the prebreakdown flow in the range tested (see Fig. 12). For greater sweep angles, the vortex lift increases relatively rapidly with initial anhedral and then subsequently decreases for anhedral

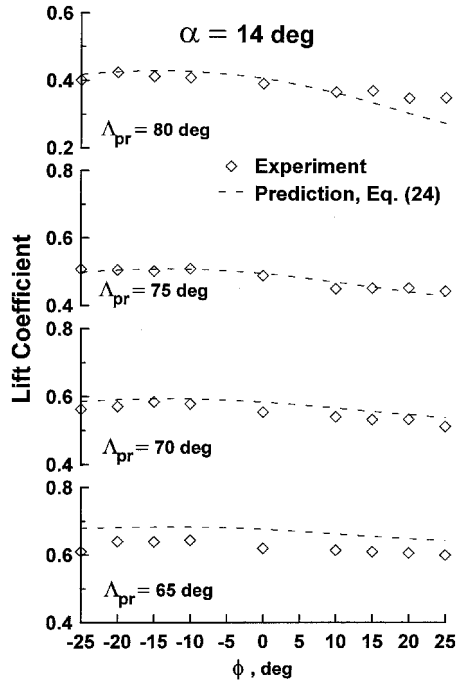

Fig. 12 Comparison of theory and experiment in effect of ϕ on lift, α = 14 deg.

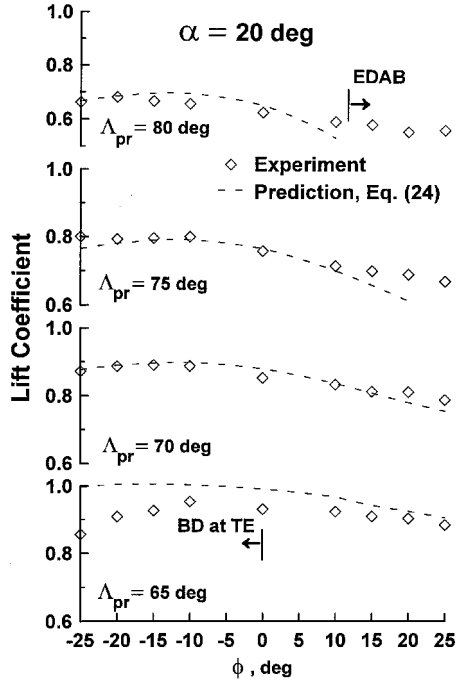

Fig. 13 Comparison of theory and experiment in effect of ϕ on lift, α = 20 deg.

angles larger than 10 deg, whereas C_{Lp} increases continuously, if weakly. For anhedral angles greater than $\sim\phi = -10$ deg, the net effect of the variation of the lift constituents results in C_{Lnp} varying slightly for $\phi < -10$ deg, as seen in Figs. 12–14.

Equations (23) and (24), as well as Fig. 14, show that effectiveness of anhedral/deg reduces as anhedral increases; i.e., small anhedral angles (less than 10 deg) generate larger lift increases relative to the deflection angle ($\Delta C_L/\Delta\phi$) than do large anhedral angles. This is shown explicitly in Fig. 15, where $\Delta C_L/\Delta\phi$ is presented as a function of ϕ. This figure shows that the prediction method is capable of predicting the sensitivity of lift to anhedral in both related trends and magnitude within the experimental data accuracy.

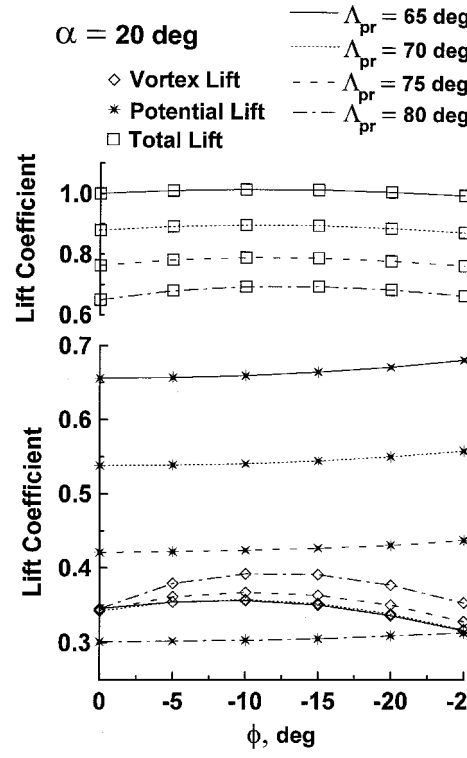

Fig. 14 Theoretical effects of sweep and anhedral on vortex lift, potential lift, and total lift.

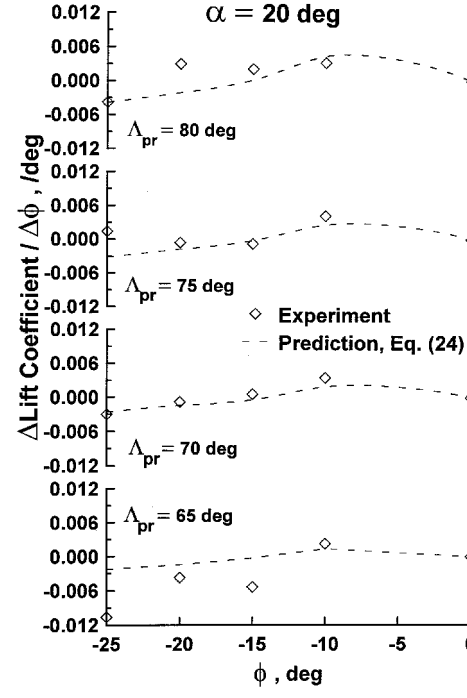

Fig. 15 Theoretical and experimental comparison of the sensitivity of lift to anhedral.

It should be noted that the present prediction method is only as accurate as the limitations of the methodologies on which it is based. Considering the suction analogy, this generally implies delta wing AR < 2 and a sharp leading edge unless partial separation effects are accounted for. Ericsson's[8] effective leading-edge sweep concept may lose applicability for large dihedral angles, as observed by Stephen.[13] Agreement between the prediction method and experiment for all presented anhedral cases is good, whereas accuracy deteriorates for increasing Λ_{pr} and dihedral. It may thus be implied

that the dihedral limitations of the method are due to the effective sweep concept no longer being representative for delta wings with large sweep and dihedral. As the experimentally determined, asymmetry boundary is reasonably coincident with the α at which the dihedral predictions break down, this asymmetry boundary forms a convenient empirical applicability boundary for the method.

Concluding Remarks

A semi-empirical method is presented that predicts the lift of slender delta wings with constant anhedral or dihedral. The formulation is based on the leading-edge suction analogy. The disparate effects of anhedral and dihedral on vortex lift are estimated using the interpretation of wing roll as a change in effective leading-edge sweep. The attached flow lift component is estimated using an apparent mass expression, derived for a V wing. Comparisons of the method with experimental data show encouraging agreement.

Acknowledgment

The author would like to express his gratitude to Murray Tobak for his helpful suggestions, particularly regarding the application of the asymmetry boundaries.

References

[1]Polhamus, E. C., "A Concept of the Vortex Lift of Sharp-Edge Delta Wings Based on a Leading-Edge Suction Analogy," NASA TN D-3767, Oct. 1966.

[2]Rom, J., "High Angle of Attack Aerodynamics," Springer–Verlag, New York, 1991, pp. 177–245.

[3]Kandil, O. A., Mook, D. T., and Nayfeh, A. H., "Nonlinear Prediction of the Aerodynamic Loads on Lifting Surfaces," *Journal of Aircraft*, Vol. 13, No. 1, 1976, pp. 22–28.

[4]Lamar, J. E., and Gloss, B. B., "Subsonic Aerodynamic Characteristics of Interacting Lifting Surfaces with Separated Flow Around Sharp Edges Predicted by a Vortex Lattice Method," NASA TN D-7921, Sept. 1975.

[5]Rusak, Z., Seginer, A., and Wasserstrom, E., "Convergence Characteristics of a Vortex-Lattice Method for Nonlinear Configuration Aerodynamics," *Journal of Aircraft*, Vol. 22, No. 9, 1985, pp. 743–749.

[6]Luckring, J. M., "Comment on: 'Convergence Characteristics of a Vortex-Lattice Method for Nonlinear Configuration Aerodynamics,'" *Journal of Aircraft*, Vol. 23, No. 10, 1986, pp. 798, 799.

[7]Smith, J. H. B., "Improved Calculation of Leading Edge Separation from Slender Delta Wings," Royal Aircraft Establishment, TR 6607, Farnborough, England, UK, March 1966.

[8]Ericsson, L. E., "The Fluid Mechanics of Slender Wing Rock," *Journal of Aircraft*, Vol. 21, No. 5, 1984, pp. 322–328.

[9]Letcher, J. S., Jr., "V-Wings and Diamond Ring-Wings of Minimum Induced Drag," *Journal of Aircraft*, Vol. 9, No. 8, 1972, pp. 605–607.

[10]Jones, R. T., "Properties of Low Aspect Ratio Wings at Speeds Below and Above the Speed of Sound," NACA Rept. 835, 1946, pp. 59–63.

[11]Lowson, M. V., "Minimum Induced Drag for Wings with Spanwise Camber," *Journal of Aircraft*, Vol. 27, No. 7, 1990, pp. 627–631.

[12]Traub, L. W., "Prediction of Delta Wing Leading-Edge Vortex Circulation and Lift-Curve Slope," *Journal of Aircraft*, Vol. 34, No. 3, 1997, pp. 450–452.

[13]Stephen, E. J., "Analysis of Rolled Delta Wing Flows Using Effective Sweep and Attack Angles," *Journal of Aircraft*, Vol. 32, No. 5, 1995, pp. 978–984.

[14]Purvis, J. W., "Analytical Prediction of Vortex Lift," *Journal of Aircraft*, Vol. 18, No. 4, 1981, pp. 225–230.

[15]Stahl, W. H., Mahmood, M., and Asghar, A., "Experimental Investigations of the Vortex Flow on Delta Wings at High Incidence," *AIAA Journal*, Vol. 30, No. 4, 1992, pp. 1027–1032.

[16]Ng, T. T., and Malcolm, G. N., "Effect of Leading Edge Roundness on a Delta Wing in Wing-Rock Motion," AIAA Paper 90-3080, Aug. 1990.

[17]Squire, L. C., "Camber Effects on the Non-Linear Lift of Slender Wings with Sharp Leading Edges," CP 924, Aeronautical Research Council, London, Jan. 1966.